AIR FORCE REPORT NO.
SAMSO-TR-67-60

AEROSPACE REPORT NO.
TR-0158(3250-10)-7

Effect of Purity and Temperature on Dynamic Microstrain of Niobium (Cb)

JULY 1967

Prepared by R. D. CARNAHAN
Materials Sciences Laboratory
Laboratory Operations
AEROSPACE CORPORATION
and R. J. ARSENAULT and G. A. STONE

Prepared for SPACE AND MISSILE SYSTEMS ORGANIZATION
AIR FORCE SYSTEMS COMMAND
LOS ANGELES AIR FORCE STATION
Los Angeles, California

Air Force Report No.
SAMSO-TR-67-60

Aerospace Report No.
TR-0158(3250-10)-7

EFFECT OF PURITY AND TEMPERATURE ON DYNAMIC MICROSTRAIN OF NIOBIUM (Cb)

Prepared by

R. D. Carnahan
Materials Sciences Laboratory

and

R. J. Arsenault and G. A. Stone

Laboratory Operations
AEROSPACE CORPORATION

July 1967

Prepared for

SPACE AND MISSILE SYSTEMS ORGANIZATION
AIR FORCE SYSTEMS COMMAND
LOS ANGELES AIR FORCE STATION
Los Angeles, California

FOREWORD

This report is published by the Aerospace Corporation, El Segundo, California under Air Force Contract F04695-67-C-0158.

This report, which documents research carried out from August 1965 through February 1967, was submitted on 9 October 1967 to Captain William D. Bryden, SMTRE, for review and approval.

The affiliations of the authors are as follows:

R. D. Carnahan, Aerospace Corporation
R. J. Arsenault, University of Maryland
G. A. Stone, Franklin Institute

Approved

W. C. Riley, Director
Materials Sciences Laboratory

Publication of this report does not constitute Air Force approval of the report's findings or conclusions. It is published only for the exchange and stimulation of ideas.

Willaim D. Bryden, Jr., Capt., USAF
Project Officer

ABSTRACT

An experimental technique has been developed for a dynamic tensile stress-strain test in which plastic strain is measured continuously throughout the microstrain region extending through the macroflow region to total deformations of 5%. The tests were carried out on Nb samples having interstitial impurity levels of 160 and ~800 ppm at temperatures ranging from room temperature down to 100°K. A band spectrum of activation energies was obtained from calculations based on the measured activation volumes and temperature dependence of flow stress. The inability to predict such a phenomenon on the basis of a single rate-controlling process has led to the proposal that several sequential rate-controlling dislocation mechanisms are operative in the preyield microstrain region. These are thought to be the motion of geometrical kinks, the formation of double kinks in edges, and finally, in the macrostrain region, the formation of double kinks in screws. In less pure Nb the effect of interstitial impurities is shown to be dominant in the microstrain region a result which suggests that a fourth mechanism is overcoming interstitial barriers rather than the motion of geometrical kinks and formation of double kinks in edge dislocations.

BLANK PAGE

CONTENTS

FIGURES

TABLE

I. INTRODUCTION

The fundamental aim of most mechanical properties studies of crystalline solids is to determine the dislocation mechanisms responsible for plastic behavior. The extension of such studies to the region of preyield microstrain behavior has received renewed attention in the past few years as the details of macroscopic flow behavior have become better understood. For the most part, microstrain studies have been carried out using one of two variations of a single experimental technique (Ref. 1). The first method involves loading the sample at a constant extension rate to a predetermined stress level (less than the macroscopic yield stress), instantaneously unloading, and then determining the extent of plastic deformation to a sensitivity of 10^{-6}. The microscopic stress-strain curve is then constructed from the results of a repeated series of such measurements, each of which involves loading to an incrementally higher stress level, by relating the accumulated plastic microstrain for each step to the maximum applied stress in that step. The second variation, also carried out by stepwise increases in stress, measures the total strain to a sensitivity of $\sim 10^{-6}$ and relates the maximum stress to the area of closed hysteresis loops that are generated under certain conditions (namely, prestrained samples). The foregoing methods have yielded interesting information about the nature of preyield deformation and plastic response to stresses below the yield stress, but they have certain disadvantages for studying the dynamic behavior of dislocations.

In the first method it is physically impossible to specify a plastic strain rate, inasmuch as the test sample is reexposed, as it is loaded to its maximum stress in a particular step, to lower stresses at which flow will take place. The strain corresponding to a given stress level on the stress-microstrain curve generated by this technique will then always be greater than that at the corresponding stress level of a truly dynamic test carried out at the same extension rate.

The second method has been used to obtain correlations with dynamic macroscopic flow parameters by applying dislocation damping theory to the hysteresis loop areas (Ref. 2). The approach has been used with some success, but only samples that have been prestrained a few percent can be studied. Although the stresses are below the macroscopic yield stress, the results are not necessarily applicable to determining the dynamic dislocation flow mechanisms operative in the preyield microstrain region.

In view of these limitations, it was deemed worthwhile to develop a technique for carrying out a stress-strain study which would permit quantitative determinations of the dynamic plastic flow parameters to be made at strains in the preyield microstrain region. A test was designed to permit an evaluation to be made over a wide range in plastic strain of the differential flow parameter given by

$$\left(\frac{\partial \ln \dot{\gamma}}{\partial \tau}\right)_T$$

where $\dot{\gamma}$ is the plastic strain rate, τ is the shear stress-designated as half the tensile stress σ, and T is the absolute temperature.

It has been shown that this parameter is uniquely related to the quantity known as the activation volume v, and the under specific conditions v is directly related to the activation enthalpy H of the thermally-assisted flow process (Ref. 3). By virtue of this interrelation, reasonable speculation can be made about the nature of the rate-controlling mechanisms of dislocation motion from measurements of v and H.

II. EXPERIMENTAL METHOD

The technique used in this study involved the determination of the tensile stress-strain curve in a dynamic (continuous extension) test such that the total strain (elastic plus plastic) was measured continuously to a sensitivity of 2×10^{-6}. This was accomplished as follows: Two foil strain gages were bonded to the sample and two inactive gages bonded to a dummy sample suspended adjacent to the test sample in order to provide the four arms of a standard bridge circuit. Sample alignment was checked by using the gages as adjacent arms of the bridge to indicate the existence of a bending stress, which could then be removed by adjusting the sample. The bridge voltage signal produced by a strain was amplified and fed to a voltage-frequency converter and thence to a combination of frequency counter, digital clock, and printer which yielded a permanent record of total strain as a function of time. The load was measured continuously to a precision of 0.01 kg with an error of ±2% by the incorporation of an auxiliary full-scale suppression network in the Instron load measuring circuitry. This sensitivity proved essential to the determination of load drops at small strains. The load signal was recorded on the Instron chart and simultaneously fed to a digital voltmeter for recording on a second digital printer. The latter was triggered by a signal from the strain recording printer so that simultaneous tape records of load and strain on a time base were obtained for the range 1×10^{-6} to $15,000 \times 10^{-6}$.

The data was reduced to stress-strain curves by calculating the stress directly from the load and by separating the strain into plastic and elastic components using the relation

$$\epsilon_{plastic} = \epsilon_{total} - \frac{\sigma_{applied}}{E} \qquad (1)$$

where E is the elastic modulus determined under testing conditions identical to those described here. The experimental modulus value of $E = 1.04 \times 10^4$

kg/mm^2 with an estimated error of $\pm 0.0035 \times 10^4$ kg/mm^2 compares favorably with values in the literature that range from 0.870 to 1.20×10^4 kg/mm^2 (Ref. 4). The total strain was read to a precision of 2×10^{-6} for the first 1200×10^{-6} (i.e., to stresses of ~10 kg/mm^2) and to a precision of 10×10^{-6} for the remaining strain up to ~$15,000 \times 10^{-6}$ due to an instrument-imposed requirement to change sensitivity range in the voltage-frequency converter. (The error is estimated to be no worse than $\pm 1 \times 10^{-6}$ at small strains, based on static load-unload measurements on similar samples.) The strain was also continuously monitored by the Instron chart. The overlap region from 1 to 1.5% plastic strain provided a check on the continuity of the two techniques. The tests were carried out to a minimum extension of 5% true plastic strain to permit comparison with published results of previous dynamic flow studies of Nb.

Nominal crosshead speeds of 0.0002 and 0.001 in./min were used with 10 to 1 rate increases to 0.002 and 0.01 in./min, respectively. True plastic strain rates were calculated throughout the entire range of strains. This proved to be an important consideration in view of the dominant elastic strain contribution to total strain, especially at small strains. The true plastic strain rates varied continuously from zero at total strains of ~50×10^{-6} to the steady-state rate governed by the crosshead speed at strains beyond ~1%. At a plastic strain of 50×10^{-6}, the plastic strain rate was found to be as much as 100 times less than the uncorrected value calculated from the crosshead speed.

The samples used in this study were prepared from two types of Nb; 0.5-in. rod of nominal 200-ppm interstitial content and 0.050-in. sheet of nominal 60-ppm interstitial content. The rod was rolled to 0.050-in. sheet and tensile samples having a gage section 0.5 in. wide by 1 in. long were machined from both supplies. The 200-ppm material used in the initial portion of the research was vacuum annealed at 1×10^{-6} Torr at various temperatures to produce the range of recrystallized grain sizes shown in Fig. 1. The 60-ppm material was vacuum annealed at 1×10^{-6} Torr for 1 hr, which yielded an average grain size of 0.18 mm. The final treatment

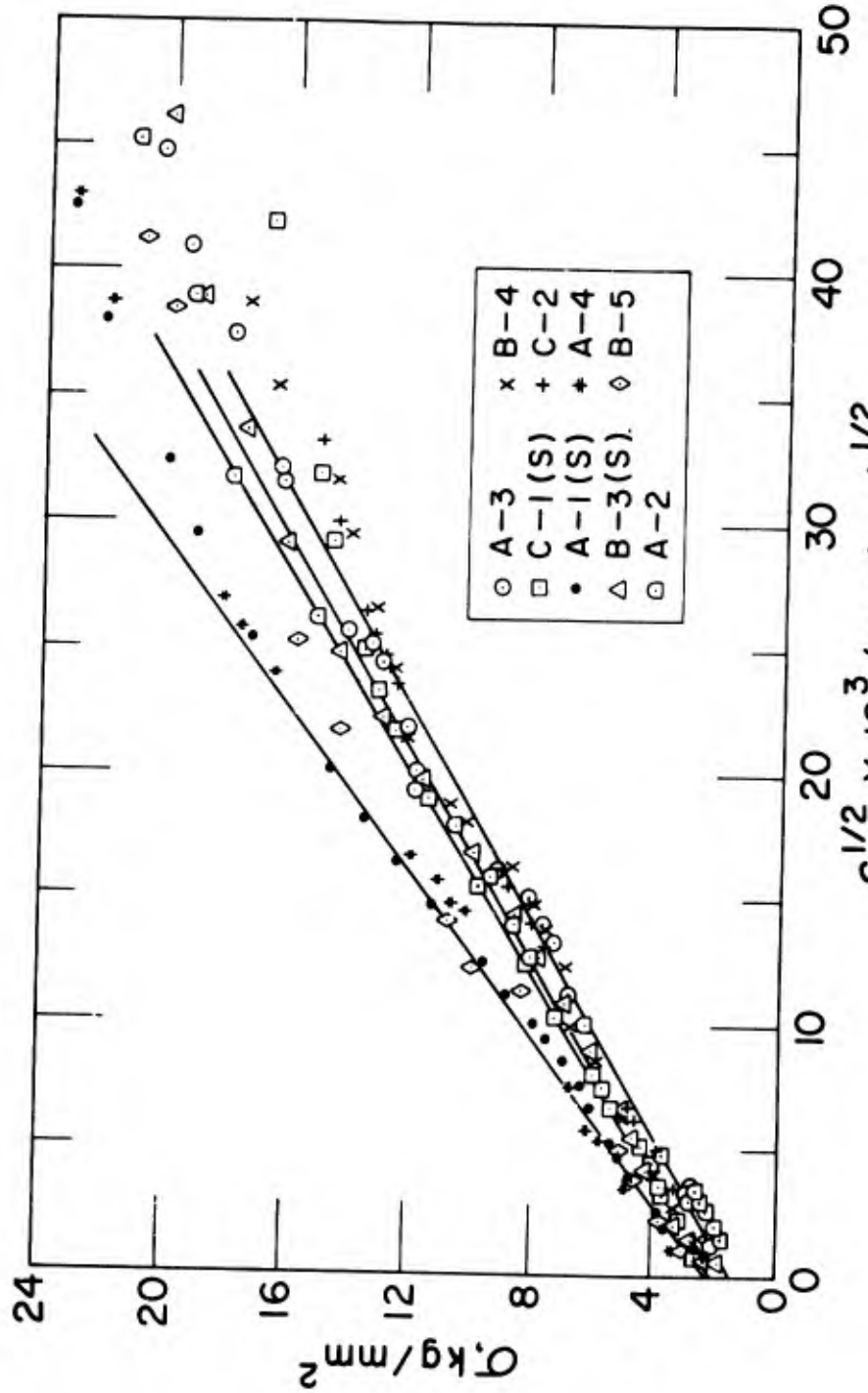

Figure 1. Parabolic Microstrain Behavior $\sigma\alpha\epsilon^{1/2}$ (Average grain diameters of samples are A = 0.015 mm, B = 0.032 mm, and C = 0.612 mm.)

involved a quench-annealing treatment consisting of annealing at 800°C in an argon atmosphere and then quenching into an ice brine solution of 5% NaOH pellets and 95% H_2O. In samples held 15 min at the annealing temperature prior to quenching, interstitial concentration increased to a level of 873 ppm for 200-ppm starting material and 772 ppm for 60-ppm starting material. Typical chemical analyses for interstitial impurities of these materials are given in Table I. Those quenched immediately after the sample

Table I. Chemical Analysis (ppm by vacuum fusion)

Samples	Carbon (C)	Hydrogen (H_2)	Nitrogen (N_2)	Oxygen (O_2)	Total
As Received	<10	18	17	<10	55
Series AA	11	49	30	682	772
Series BB	15	18	36	91	158
Series A, B, C,	10	75	245	543	873

reached temperature experienced only a small change in interstitial concentration from nominal 60 to 158 ppm. Both treatments completely suppressed the yield point and eliminated any Lüders strain. Foil strain gages measuring 5/32 in. wide by 0.25 in. long were used to ensure that the measured stress-strain behavior reflected the integrated deformation behavior of a large number of grains.

III. EXPERIMENTAL RESULTS

A preliminary investigation was undertaken to determine the effect of grain size on the microyield region. A summary of the results obtained at 296°K is contained in Fig. 1. Results of both static and dynamic tests of all three grain sizes for the 873-ppm material are plotted as flow stress versus the square root of the plastic strain. Some of the general microstrain features of Nb can be inferred from Fig. 1. The microyield stress, defined as the stress to produce a plastic deformation of 1×10^{-6}, varies from about 1.8 to 3.3 kg/mm^2, which is in excellent agreement with observations of Koppenaal and Evans (Ref. 5) for unpinned dislocations in Nb. A good linear fit to the data is obtained in all cases up to strains of about 1×10^{-3} (i.e., $\epsilon^{1/2} \sim 30 \times 10^{-3}$), which indicates agreement with the parabolic $\sigma \alpha \epsilon^{1/2}$ relationship observed in previous microstrain investigations (Refs. 6-8). Koppenaal and Evans (Ref. 5) did not observe this parabolic relationship in Nb. The slopes of these curves $d(\epsilon^{1/2})/d\sigma$ range from 1.64 to 2.15×10^{-3} mm^2/kg, and extrapolation of the plot to zero strain yields a value of 1.5 to 2.5 kg/mm^2 for the zero stress of Nb. No systematic variations in any of these features were noted with either grain size or strain rate. It was found, however, in an extension of the tests to lower temperatures, that an increase in the slope of the plots of σ versus $\epsilon^{1/2}$ resulted, as seen in Fig. 2. The slope was also found to be sensitive to the interstitial concentration; for example, at 296°K a slope of 3.7×10^{-3} mm^2/kg was found for the 772-ppm Nb and 6.25×10^{-3} mm^2/kg for the 158-ppm Nb.

In order to permit determination of the differential flow parameter at various levels of plastic strain, strain rate changes of 10 to 1 were imposed during the continuous tests. It was found to be experimentally feasible to measure the flow parameter at plastic strains as small as 38×10^{-6}. An example of the flow curve obtained in such a test is shown in Fig. 3, represented in three parts for clarity. It was necessary to make extrapolations of the experimental curves, as is usual practice for the macrostrain region, in order to determine the instantaneous values of $\Delta\sigma$ associated with the

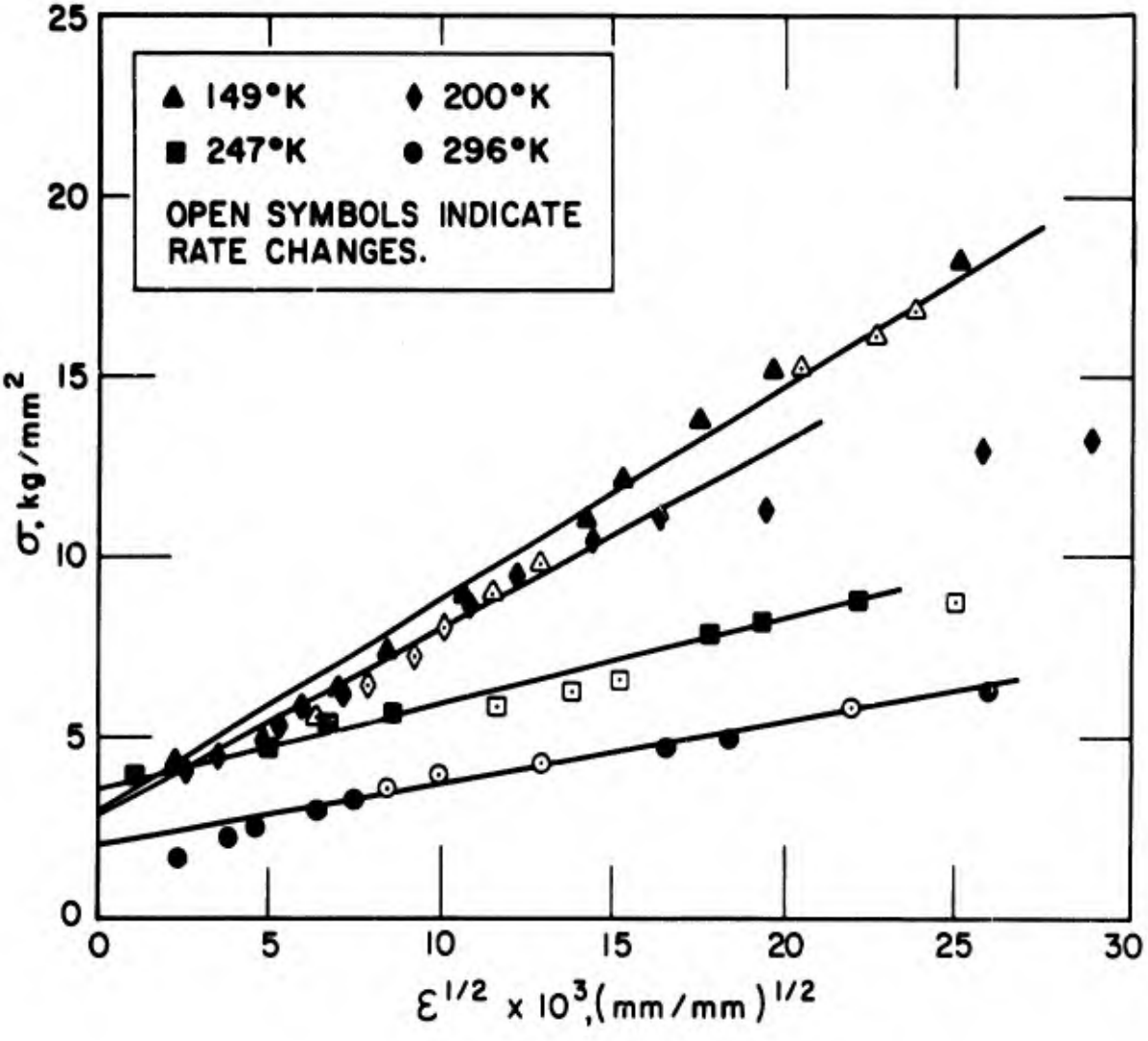

Figure 2. Temperature Dependence of Parabolic Microstrain Behavior for 158 ppm Nb.

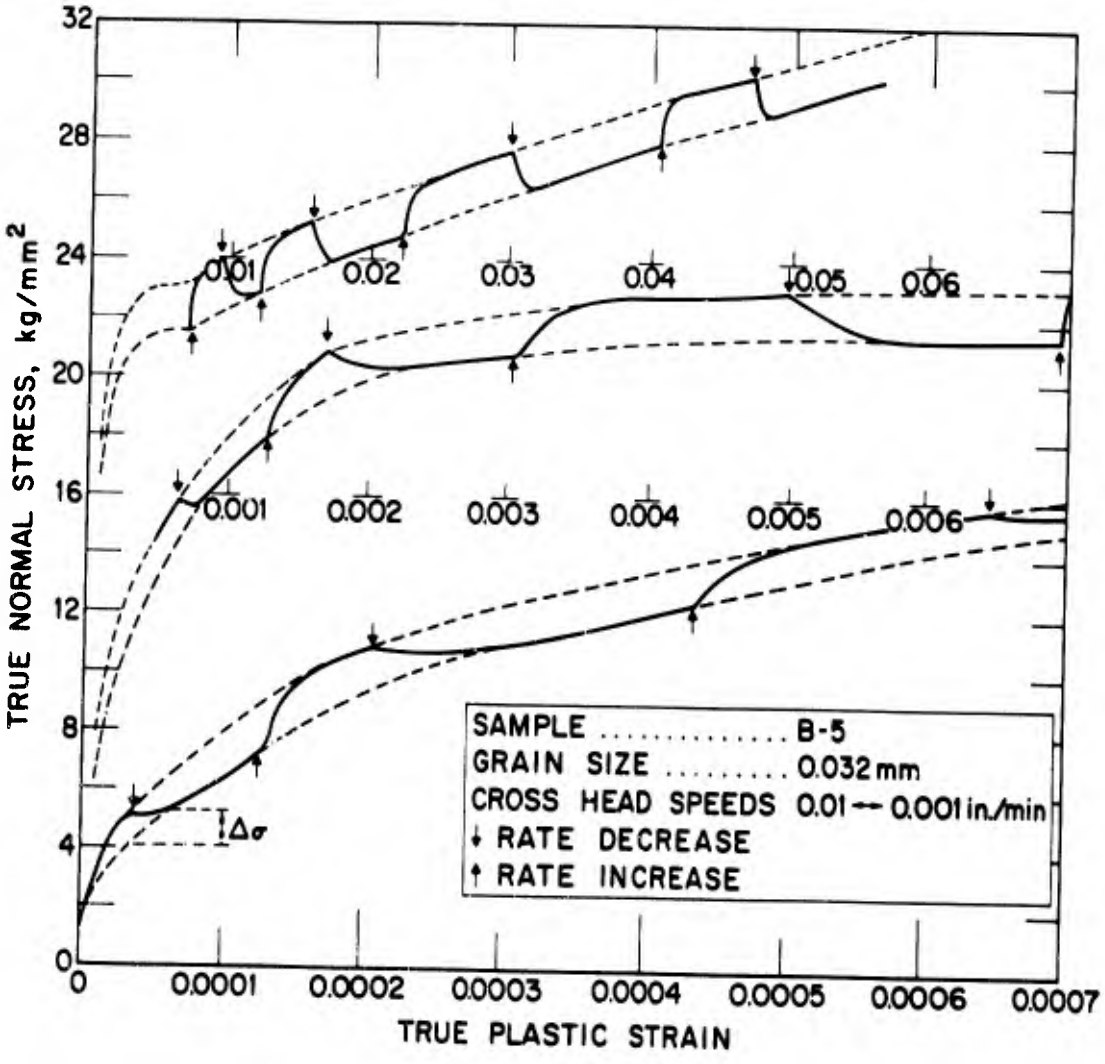

Figure 3. Dynamic Tensile Test Employing Differential Strain Rate Technique To Determine $(\partial \ln \dot{\gamma}/\partial \tau)_T$.

imposed strain rate changes. It is noted that whereas the actual stress drops obtained from the corrected flow curves (Fig. 3) are of comparable magnitude to those occuring at much larger strains, the apparent load drop associated with a rate decrease for strains up to ~1000×10^{-6} was frequently extremely small, as measured either from the Instron record or the load printout tape.

The activation volume was calculated from the flow parameter through the relation

$$v = kT\left(\frac{\partial \ln \dot{\gamma}}{\partial \tau}\right)_T \qquad (2)$$

where kT is the product of the Boltzmann's constant and the absolute temperature, $\dot{\gamma}$ is the shear strain rate, and τ is the shear stress.

Implicit in calculating v by the above equation is the fact that the density of mobile dislocations does not change when a change in strain rate is made.

The authors recognize that these measurements are made in a range in which the strain is not uniformly homogeneous and that the "mobile" dislocation density is progressively increasing from zero to an eventual steady-state value of ~10^8 lines/cm^2 in the macrostrain region. Although no direct method of verification was available it has been assumed that there is no change in the mobile dislocation density with an instantaneous change in strain rate. There must be, however, a change in this quantity between any two consecutive strain rate changes in this region of deformation. Three factors supporting this assumption are (1) the change in flow stress is measured at a constant strain by extrapolation of the flow curves, (2) the change in flow stress is the same for either an increase or a decrease in strain rate at a given strain, and (3) the flow stresses at a given strain obtained in tests run at constant strain rates yield $\Delta\sigma$'s consistent with those obtained in a differential strain rate test. There is however a normal scatter of ~5% between two curves run at a single strain rate that precludes using $\Delta\sigma$ values from two random constant strain rate tests to calculate v.

In Fig. 4, it can be seen that the activation volume is initially large and shows a decrease with increasing strain to about the range 5×10^{-4} to 1×10^{-3}, beyond which there is essentially no further strain dependence. The corresponding activation volumes for the tests summarized in Fig. 1 were in all cases lower by about 20 units of v/b^3 than those of Fig. 4 for strains larger than 10^{-4}. At strains below 10^{-4}, limited data suggests a divergence of the curves in which v increases more rapidly with decreasing strain in the more pure material.

It was also noted that the strain at which the activation volume levels out is almost independent of grain size, although there is some indication that this value is smaller for larger grain sizes. To the extreme right in Fig. 4 the data of Conrad and Stone (Ref. 9) obtained at macroscopic strains at corresponding temperatures are plotted for comparison.

The temperature dependence of the microyield stress at various strains (and of necessity various strain rates) was also determined, and is shown in Fig. 5. It is seen here that the temperature dependence of the microyield stress increases with increasing strain (Fig. 5) for samples of two extreme purity levels. At a strain of 3×10^{-3} the temperature dependence of the 158-ppm samples is the same as that for macroscopic deformation, whereas the less pure 778-ppm samples showed a temperature dependence comparable to the macroflow stress at a strain of 2×10^{-4}.

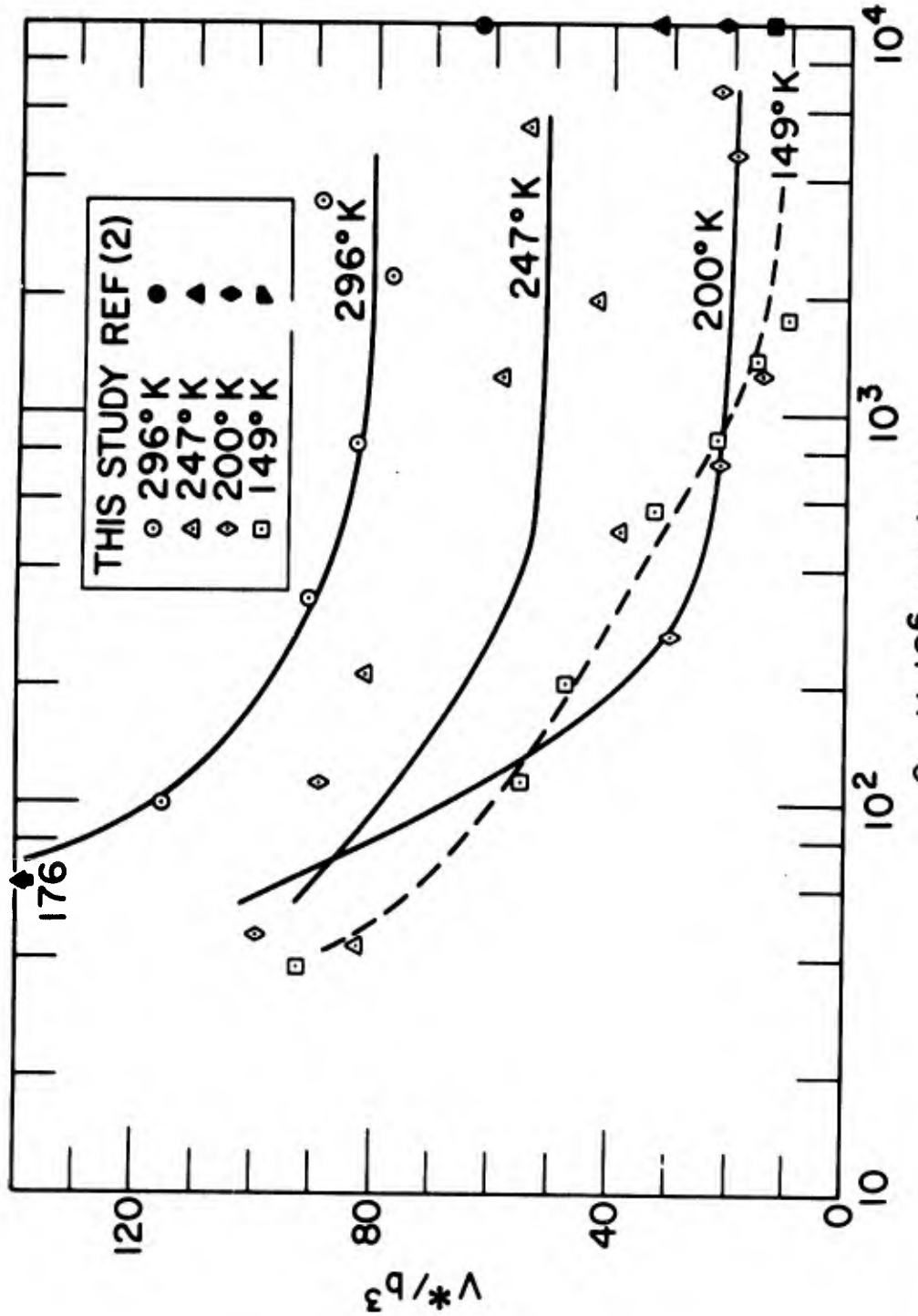

Figure 4. Variation of Activation Volume with Plastic Strain and Temperature for 158 ppm Nb.

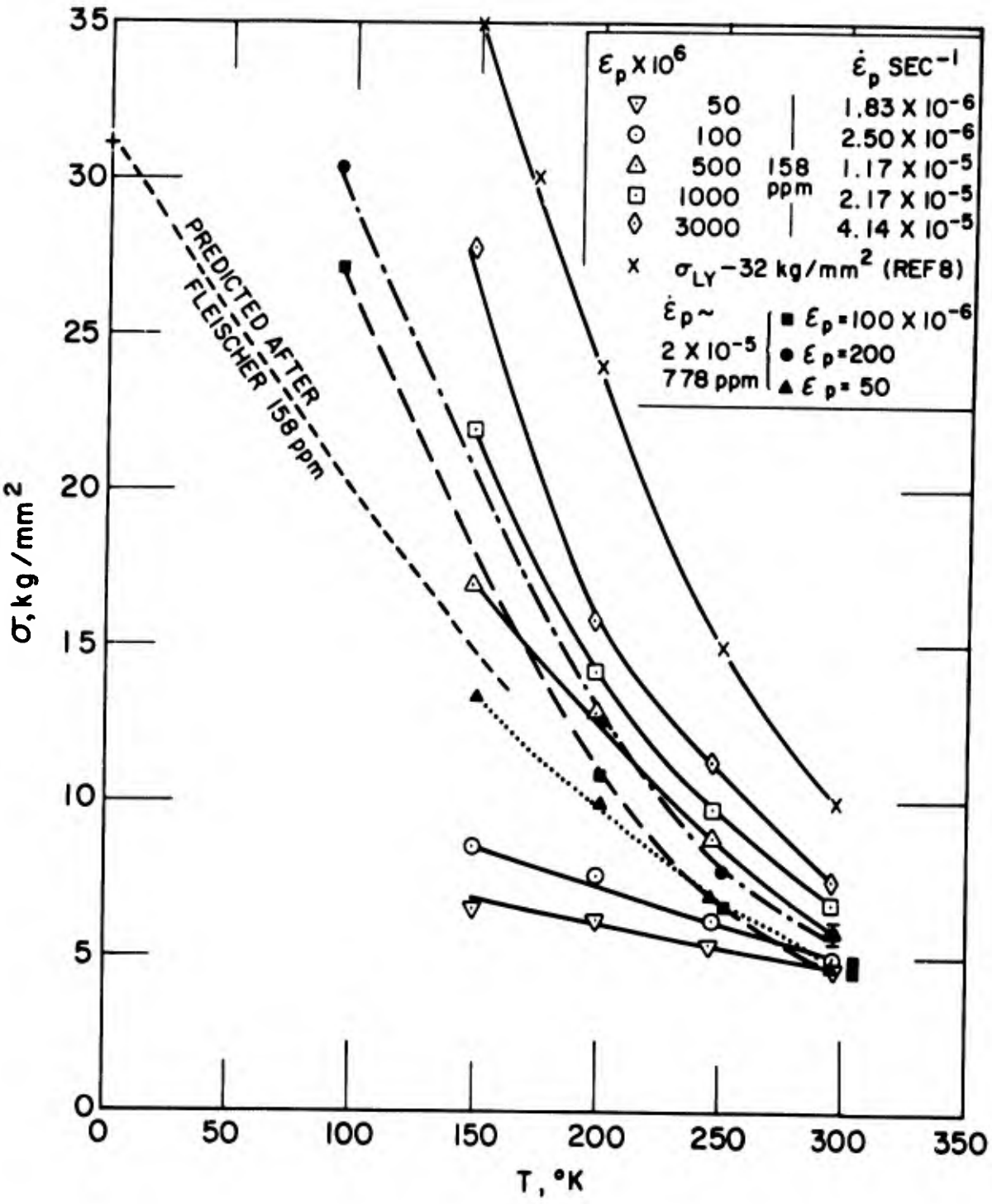

Figure 5. Temperature Dependence of Microflow Stress at Various Microstrains for Both 158- and 772-ppm Nb

BLANK PAGE

IV. DISCUSSION

The primary purpose of this investigation was to demonstrate the feasibility of a dynamic stress-strain test which would be continuous from the preyield microstrain region to macrostrains of several percent. It is believed that only by such a technique can a proper evaluation be made of the processes operative in the preyield and postyield regions of deformation and the question resolved as to whether one or more specific mechanisms is rate controlling throughout the yielding process.

The most direct manner of determining whether one or more rate controlling mechanisms is operative in the microyield region would be to determine the activation energy or activation volume as a function of effective stress. If it were determined that the results fit a single curve then there would be a strong indication that a single rate controlling mechanism was operative. To test this hypothesis it is essential to determine the effective stress, defined as the applied stress minus the athermal component of the applied stress. It is generally assumed that the athermal component is due to the long range stress fields of dislocations within the sample, which unfortunately is indeterminate in the microstrain region.

A less direct approach than the foregoing one can be used, however, by studying the temperature dependence of the activation energy. It is possible to determine the activation energy at various temperatures and strains in the microyield region by the use of the following expression (Ref. 3), which does not depend on specific knowledge of the effective stress

$$H = -vT\left(\frac{\partial \tau}{\partial T}\right)_{\dot{\gamma}} \qquad (3)$$

The temperature variation of the activation energies calculated from the data obtained in this study are shown in Fig. 6 for various levels of microstrain. Included for comparison in Fig. 6 are data obtained by Conrad and Stone (Ref. 9) from a study of macroscopic deformation of Nb. Inasmuch as a

family of curves is obtained rather than a single line it would seem that there is indeed more than one rate-controlling mechanism. A valid objection to this comparison might be made, inasmuch as the strain rates were not held constant, but since the data cannot be obtained for comparison at the same strain rate it is necessary to determine the strain-rate dependence of the relationship of H vs T. We will consider the following expression for strain rate

$$\dot{\gamma} = A \exp\left[-\frac{H_0 - \int_0^{\tau^*} v(\tau^*)\, d\tau^*}{kT}\right] \tag{4}$$

where A contains the vibrational attempt frequency, the entropy factor, the strain produced per activated event, and the number of dislocations participating in the deformation, and H_0 is the enthalpy (activation energy) at zero effective stress. For zero effective stress, Eq. (4) can be reduced to

$$H_0 = kT \ln (A/\dot{\gamma}) \tag{5}$$

For a single rate-controlling mechanism H_0 is independent of strain rate. For a factor of 10 change in strain rate, the approximate spread of strain rates over which the values shown in Fig. 6 were determined, the change of H vs T would be described by the difference between the solid line representing the maximum H and the dashed line in Fig. 6. The curves for small strains do not fit within the band defined by the differences in strain rates; this fact lends further support to the hypothesis that there is indeed more than one rate-controlling mechanism in the microyield region. Another point of significance is that H_0 for small strains is much smaller than that for macroscopic slip. An explanation for the curvature of H vs T, based on the the existence of variations in the internal stress distributions, has recently been suggested (Ref. 10).

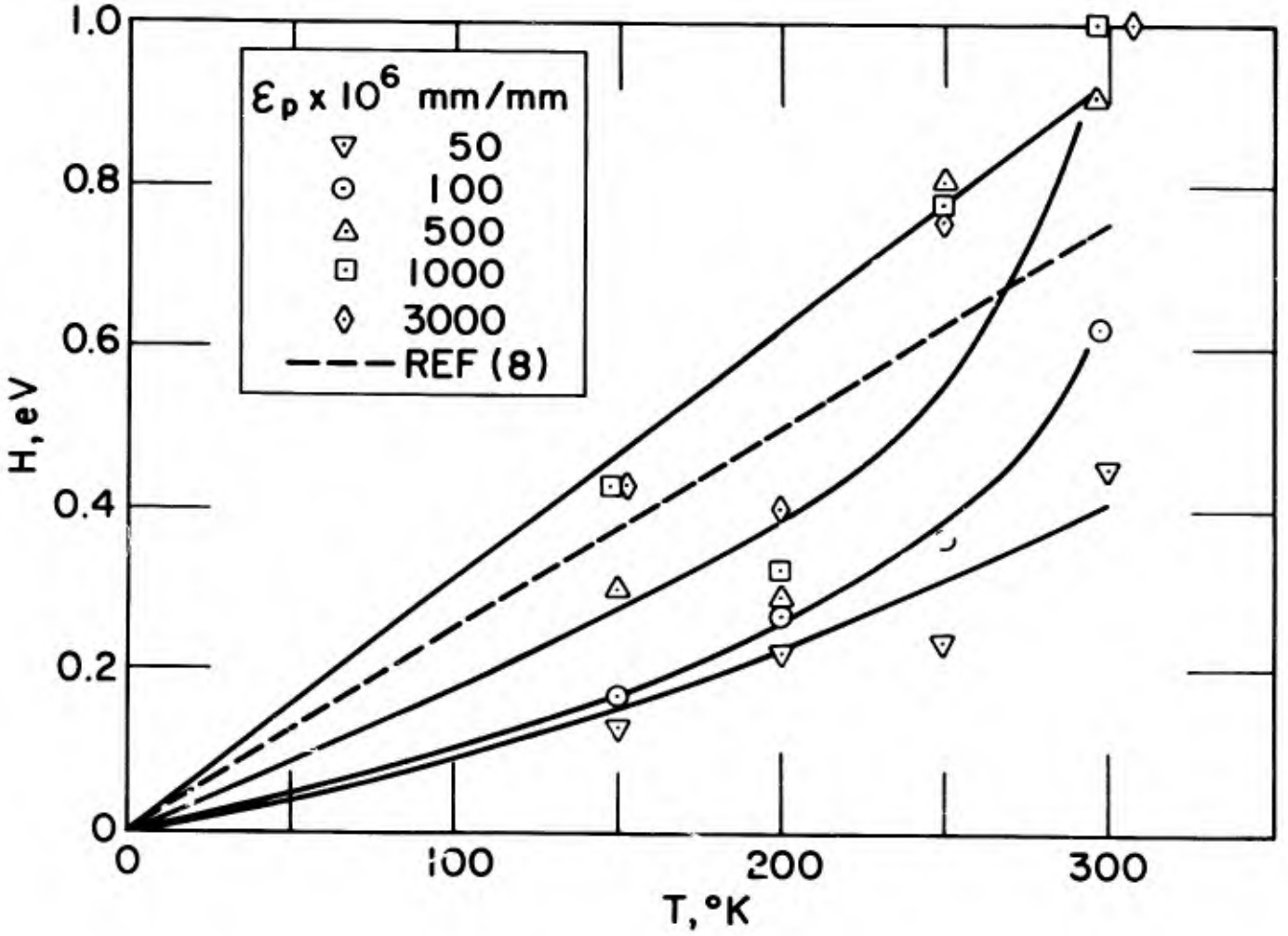

Figure o. Calculated Activation Energies vs Temperature for 158 ppm Nb at Various Microstrains.

The slope of curves of H vs T is related to the preexponential term A, and, as stated above, A is related to the density of mobile dislocations. If it is assumed that the change in the slope is due entirely to a change in the mobile dislocation density (the change in the strain per activated event is canceled by the change in the attempt frequency), the density would increase by $\sim 10^4$ for an increase of $\epsilon = 50 \times 10^{-6}$ to $\epsilon = 3 \times 10^{-3}$. A change in the density of mobile dislocations is to be expected in the microyield region, since the density of mobile dislocations at zero plastic strain is zero and the density at the macroscopic yield stress is $\sim 10^7$ to 10^8 cm^{-2}. The hypothesis that there is more than one rate-controlling mechanism in the microyield region might also be objected to on the grounds that the family of curves may be due to a difference in the density of mobile dislocations. However, if the family of curves was due to differences in mobile dislocation density, then the same value of H_0 would be obtained for each level of strain; again it should be remarked that H_0 is much smaller for small strains, a fact which further strengthens the hypothesis.

The increase in the temperature dependence of the microyield stress with an increase in the interstitial concentration can be explained in terms of the effect of interstitial impurities on the various rate-controlling mechanisms that may be operative in the microyield region. The most probable dislocation mechanisms and their sequence of operation as rate-controlling mechanisms are the following: The first mechanism producing plastic deformation is the motion of geometrical kinks, in both edge and screw dislocations. This mechanism is followed by the formation of double kinks in the edge components of dislocations. The relative ease with which double kinks form in edges by contrast with the formation of screw dislocations is due to the smaller Peierl's stress associated with edge dislocations (Ref. 11). Finally it is necessary for the formation of double kinks in the screw components of dislocations to occur, which is thought to be the rate-controlling mechanism (Ref. 11) for macroscopic deformation. This sequence of events is depicted schematically in Fig. 7. Several models or mechanisms (Refs. 12-14) have been proposed in which interstitial atoms act as barriers to the

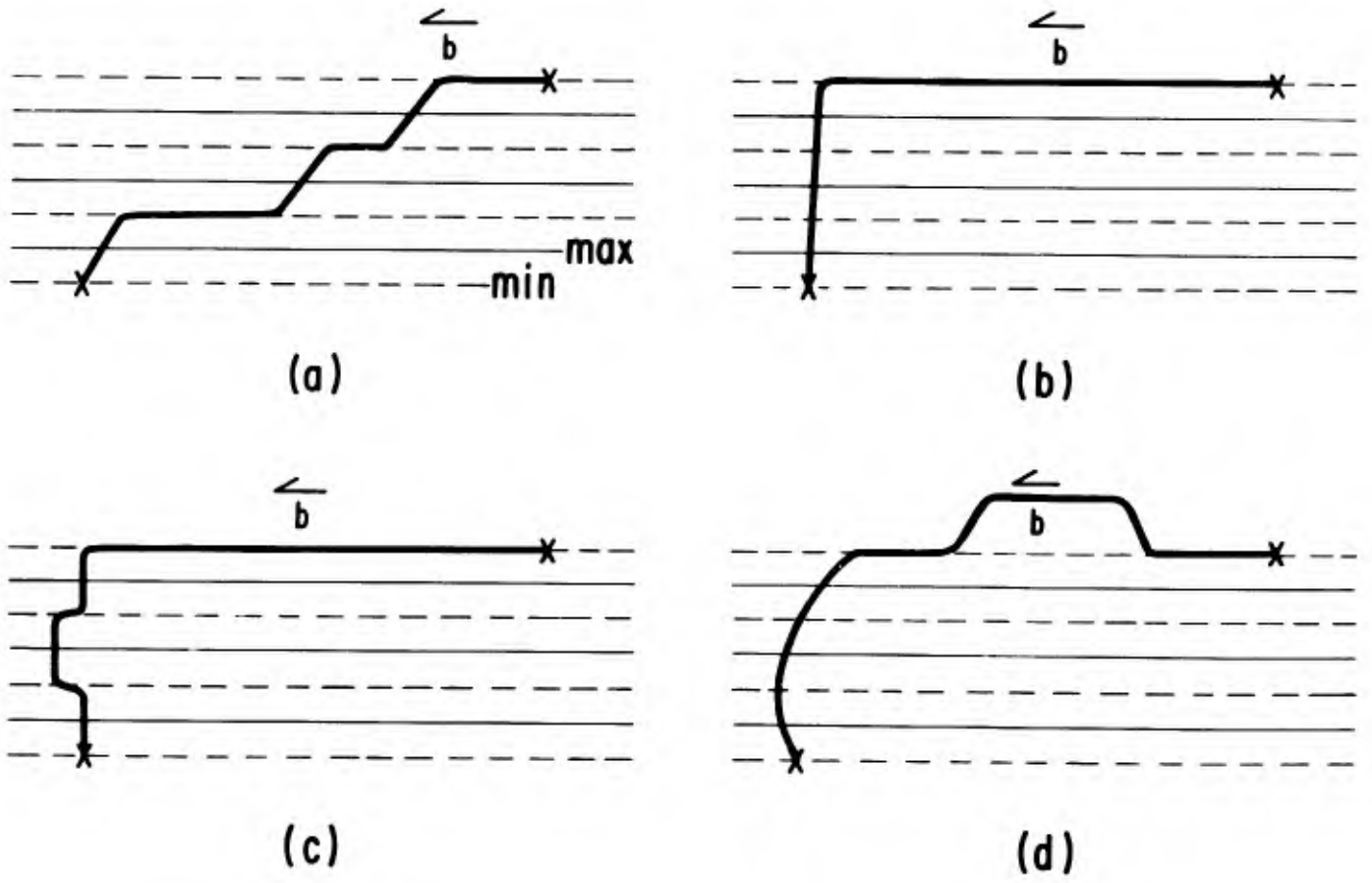

Figure 7. Schematic Model for Dislocation Motion (a. Geometrical Kink, b. Pure Edge and Screw Components, c. Double Kink Formation of Edge Component, and d. Double Kink Formation on Screw Component).

motion of dislocations. Fleischer (Ref. 14) has developed a generalized model for the interaction force between a defect and a moving dislocation in which the defect must produce a tetragonal distortion in the lattice, a condition satisfied by interstitial atoms in bcc metals. From the force-distance relationship proposed by Fleischer the following expressions for H and v are obtained:

$$H = H_0 \left[1 - \left(\frac{\tau^*}{\tau_0^*} \right)^{1/2} \right]^2 \tag{6}$$

and

$$v = \frac{H_0}{\tau_0^*} \left[\left(\frac{\tau_0^*}{\tau} \right)^{1/2} - 1 \right] \tag{7}$$

where τ_0^* is the effective stress at absolute zero. The test of this theory requires the determination of the variation of the activation parameters with effective stress in order to obtain a plot of τ vs T. Once again, however, the ambiguity of an undefined internal stress (athermal component) precludes making the necessary calculations. We can, however, make use of the expression given by Fleischer for the flow stress at absolute zero in order to obtain limiting values for the two purity levels.

In calculating τ_0 for interstitial concentrations of 158 and 772 ppm it is assumed that the tetragonality strain factor ΔE is 0.4, and that the interstitials are randomly oriented and in solution due to quenching. Further, since the dominant strengthening role of H_2 and N_2 in Nb is believed due to the formation of precipitates, both are disregarded in the calculation. The appropriate atomic fraction of combined C and O_2 interstitials is 6.44×10^{-4} and 4.04×10^{-3}, respectively, in Nb having 158 and 772 ppm total interstitials by weight. The value of τ_0 for the 158-ppm Nb plotted in Fig. 5 has been

increased by 5 kg/mm^2, the apparent athermal component deduced from the asymptote for the family of curves shown. A curve synthesized for the 158-ppm Nb lies between the 158-ppm experimental curves for 1×10^{-4} and 5×10^{-4}. Although the calculated σ_0 value for the 778-ppm material, 69 kg/mm^2, does not fit on the curve, it is still in the preyield region, since it falls below the extrapolated σ_0 value (114 kg/mm^2). This value is obtained from a summary of lower yield and flow stress data for Nb as a function of temperature, corrected for the athermal component of the stress (Ref. 9). The important result of this simple analysis is that it indicates that the interaction between a dislocation and the interstitial atoms may be a rate-controlling mechanism during some portion of the preyield region, although the presence of interstitial atoms does not appear to affect the mechanism for macroscopic flow.

Let us now consider the results of the analysis in terms of the proposed mechanisms. The motion of geometrical kinks requires a finite stress, but, if the interstitial impurity concentration is sufficient, it is then possible that the interstitials will constitute a large barrier which prevents the geometrical kink mechanism from being rate controlling. The dislocation will probably still move from position a to b as described in Fig. 7. After the dislocation line has reached position b, double kink formation on the edge component will become rate controlling if the barrier magnitude is larger than that for impurities; the sequence of operation of the mechanisms will then be as described before. However, if the interstitial concentration is sufficiently large to establish a barrier larger than that due to double kink formation on the edge components, then the rate-controlling mechanism for the entire microstrain region will be the overcoming of the barrier due to interstitial atoms. The important consequence is that the amount of strain, i. e., microstrain prior to macroscopic deformation, will be extremely small. The experimental results indeed indicate that as the interstitial concentration is increased, the amount of strain prior to macroscopic flow decreases. Furthermore, if the interstitial mechanism were the rate-controlling mechanism for microscopic flow, there would be little or no preyield microstrain.

The reduction due to interstitial impurities in the extent of deformation that can be attributed to the various dislocation mechanisms results directly in the observed increase in temperature dependence of the microyield stress and also in an increase in slope of the plots of σ vs $\epsilon^{1/2}$.

In Fig. 2 the experimental stress-strain behavior was parabolic with $\sigma \alpha \epsilon^{1/2}$ for plastic strains up to about 0.1%, the region of the lower yield point for unquenched Nb. Brown and Lukens (Ref. 7) proposed a model based on dislocation pile-ups from which they were able to obtain a parabolic relationship of the type $\sigma \alpha \epsilon^{1/2}$. There are, however, several dubious assumptions associated with this model, which is basically a work-hardening model. Kossowsky and Brown[15] have pointed out in a recent paper that all theories (Refs. 16-19) of work hardening indicate that the maximum rate of work hardening is approximately $\mu/300$, in contrast with values of $\sim \mu/30$ obtained in this study. The observation $\sigma \alpha \epsilon^{1/2}$ cannot, therefore, be explained in terms of a dislocation interaction model, i.e., a work-hardening model. The slopes of the plots of σ versus $\epsilon^{1/2}$ also increase with decreasing temperature, again contrary to the work-hardening theories, all of which predict that the rate of work hardening is to a first approximation independent of temperature. At present it appears that there is no acceptable explanation of the observed parabolic relationship.

A possible mechanism for deviation from the parabolic relationship in the region of macroscopic yielding is the rapid increase in density of mobile dislocations. An increase in the density of mobile dislocations will result in a reduction in the velocity at which the dislocations must move in order to maintain a given strain rate, and as the velocity decreases the stress will also decrease. Similarly, it has been observed in Be (Ref. 6) that when profuse cross slip occurred, the parabolic relationship was no longer valid. It is assumed that when cross slip occurs dislocation multiplication also occurs.

V. CONCLUSIONS

A detailed study of the dynamic stress-strain behavior of Nb has been carried out over an extended range of plastic deformation from preyield microstrains of 1×10^{-6} to 5% plastic strain. Using Nb of two purity levels, 158 and 772 ppm interstitial impurities, the activation energies and activation volumes were determined by means of differential strain rate tests carried out at temperatures ranging from 100 to 300°K. The activation volumes were found to be strain sensitive; v took on large values at small strains and decreased asymptotically toward the macroscopic strain values at a total strain of about 10^{-3}. The microflow stress was found to show an increasingly stronger temperature dependence as strain increased up to a total strain of about 10^{-3}, where the dependence parallels that of macroflow. An increase in interstitial impurity concentration caused an increase in temperature dependence of the flow stress, so that the curve for a strain of 2×10^{-4} coincided with that for 10^{-3} in the more pure Nb. A band spectrum calculated from the experimental data showed that the activation energy H_0 gradually increases from about 0.4 to 1.0 eV as strain increases to 10^{-3}.

A plausible explanation of this behavior takes into account the fact that several types of dislocation motion occur during the preyield region, which constitutes in essence an exhaustion sequence (Ref. 20) in which several rate-controlling processes are operative. First the simplest form of dislocation motion, the movement of geometrical kinks, occurs. On exhaustion of geometrical kinks, the formation of double kinks in edge dislocations occurs, and ultimately the formation of double kinks in screws begins with the onset of macroscopic deformation. Interstitial impurities, by virtue of interaction due to their tetragonal distortion, will limit the extent of strain in the microstrain region and introduce a fourth rate-controlling mechanism, that of overcoming interstitial barriers. A simplified analysis based on Fleischer's theory suggests that this mechanism is operative in the region of deformation of 10^{-4} or lower for the interstitial concentration of the Nb used in this investigation.

Parabolic microstrain behavior was observed only up to deformations of 10^{-3} in all cases, which suggests that this mechanism applies only in the preyield exhaustion region and no longer holds when multiplication by cross slip begins.

REFERENCES

1. R. D. Carnahan, J. Metals, 12, 16, 990 (1964).
2. J. Roberts and N. Brown, Trans. AIME, No. 218, 454 (1960).
3. H. Conrad and H. Wiedersich, Acta Met., 8, 128 (1960).
4. D. P. Laverty and E. B. Evans, Columbium Metallurgy, Interscience Publishers, New York (1961), pp 299-306.
5. T. J. Koppenaal and P. R. V. Evans, J. Inst. Metals, 92, 225 (1964).
6. W. Bonfield and C. H. Li, Acta Met., 12, 557 (1964).
7. N. Brown and K. F. Lukens, Jr., Acta Met., 9, 106 (1961).
8. T. J. Koppenaal, Acta Met., 11, 537 (1963).
9. G. A. Stone and H. C. Conrad, Acta Met., 12, 577 (1964).
10. R. J. Arsenault, Submitted to Phil. Mag.
11. R. J. Arsenault, Acta Met., 14, 831 (1966).
12. A. H. Cottrell and M. A. Jaswon, Proc. Roy. Soc., A 199, 104 (1949).
13. G. Schoeck and H. Seeger, Acta Met., 7, 469 (1959).
14. R. L. Fleischer, Acta Met., 10, 835 (1962); J. Appl. Phys., 33, 3504 (1962).
15. R. Kossowsky and N. Brown, Acta Met., 14, 131 (1966).
16. A. Seeger, Dislocations and Mechanical Properties of Crystals, J. Wiley and Sons, N. Y. (1956) 243-329.
17. G. I. Taylor, Proc. Roy. Soc. A., 145, 362 (1934).
18. P. B. Hirsch, Discussions Faraday Soc., 38, 111 (1964).
19. D. Kuhlam-Wilsdorf, Trans. Met. Soc. AIME, 224, 1047 (1962).
20. R. D. Carnahan and J. E. White, Phil. Mag., 10, 513 (1964).

UNCLASSIFIED

Security Classification

DOCUMENT CONTROL DATA - R&D

(Security classification of title, body of abstract and indexing annotation must be entered when the overall report is classified)

1 ORIGINATING ACTIVITY (Corporate author)

Aerospace Corporation
El Segundo, California

2a REPORT SECURITY CLASSIFICATION

Unclassified

2b GROUP

3 REPORT TITLE

EFFECT OF PURITY AND TEMPERATURE ON DYNAMIC MICROSTRAIN OF NIOBIUM (Cb)

4 DESCRIPTIVE NOTES *(Type of report and inclusive dates)*

5 AUTHOR(S) *(Last name, first name, initial)*

Carnahan, Robert D., Arsenault, Richard J., Stone, Glen A.

6 REPORT DATE	7a TOTAL NO OF PAGES	7b NO OF REFS
May 1967	29	20

8a CONTRACT OR GRANT NO	9a ORIGINATOR'S REPORT NUMBER(S)
F04695-67-0158	
b. PROJECT NO	TR-0158(3250-10)-7
c	9b OTHER REPORT NO(S) *(Any other numbers that may be assigned this report)*
d	SAMSO-TR-67-60

10 AVAILABILITY/LIMITATION NOTICES

This document has been approved for public release and sale; its distribution is unlimited.

11 SUPPLEMENTARY NOTES	12 SPONSORING MILITARY ACTIVITY
	Space Systems Division Air Force Systems Command Los Angeles, California

13 ABSTRACT

An experimental technique has been developed for a dynamic tensile stress-strain test in which plastic strain is measured continuously throughout the microstrain region extending through the macroflow region to total deformations of 5%. The tests were carried out on Nb samples having interstitial impurity levels of 160 and ~800 ppm at temperatures ranging from room temperature down to 100°K. A band spectrum of activation energies was obtained from calculations based on the measured activation volumes and temperature dependence of flow stress. The inability to predict such a phenomenon on the basis of a single rate-controlling process has led to the proposal that several sequential rate-controlling dislocation mechanisms are operative in the preyield microstrain region. These are thought to be the motion of geometrical kinks, the formation of double kinks in edges, and finally, in the macrostrain region, the formation of double kinks in screws. In less pure Nb the effect of interstitial impurities is shown to be dominant in the microstrain region a result which suggests that a fourth mechanism is overcoming interstitial barriers rather than the motion geometrical kinks and formation of double kinks in edge dislocations.

DD FORM 1473 (FACSIMILE)

UNCLASSIFIED

Security Classification

14 KEY WORDS

Niobium
Microstrain
Dynamic microplasticity
Dislocation mechanisms (thermal)
Interstitial hardening
Preyield deformation

Abstract (Continued)